

ROCK TYPING IN GEOTHERMAL RESERVOIRS, CHALLENGING THE COMPLEXITY

Angela M. Prieto¹, Philipp Mielke², Rosalind Archer¹, John S. Sneider³, Santanu Misra⁴

¹University of Auckland, Department of Engineering Science, Level 3, 70 Symonds St, Auckland, New Zealand

²Darmstadt University of Technology, Schnittspahnstrasse 9, D - 64287 Darmstadt, Germany

³Sneider Exploration, Inc., League City, TX 77573, United States

⁴GNS Science, Avalon 5010, Wellington, New Zealand

apri049@aucklanduni.ac.nz

Keywords: Petrophysical properties, geothermal reservoir characterisation, rock typing, New Zealand.

ABSTRACT

In order to simulate the behaviour of a geothermal system for field management purposes, a numerical model is initialised based on conceptual models that capture the initial state of the reservoir, integrating the current knowledge of the system and its dynamics.

Geothermal reservoirs are dynamic systems, where continuous fluid and heat flow affects the reservoir chemical and stress equilibria leading to precipitation or dissolution of minerals and changes in the pore geometry over the lifetime of geothermal activity. The speed and intensity of these changes depend on the rock's capacity to store and transfer fluids coupled with the physicochemical properties of the fluids and the pressure and temperature of the system. The rocks resulting from these processes are characterized by a wide range of petrophysical properties, which are seldom represented by traditional classification of rocks based on individual geological parameters of genesis, lithology or composition. As a consequence, translating these properties into quantitative inputs for numerical models remains a challenge.

This paper presents the conventional approach to petrophysical characterisation of geothermal reservoirs in New Zealand, and proposes the use of textural descriptors as part of a rock typing technique aimed at facilitating the quantification and use of measured petrophysical properties in the reservoir modelling workflow.

1. INTRODUCTION

Geothermal systems constitute one of New Zealand's most valued natural resource having provided hot fluids to generate electricity for residential, commercial and industrial consumption for over 50 years, and thermal features that are part of the local tradition. Currently, geothermal energy covers about 14% of the national electricity supply (Ministry of Business Innovation and Employment, 2013) with a projected increase to 25% by 2025 (Bromley, 2012).

Most of New Zealand's geothermal systems are located in the Taupo Volcanic Zone (TVZ), a rift structure in the North Island formed within the volcanic arc generated by the active convergence of the Pacific plate beneath the Australian plate (Wilson et al., 1995) (inset Figure 1).

In order to use and manage these resources, geological, geophysical and geochemical surveys are carried out in geothermal areas, paying especial attention to

manifestations of the deep resource, e.g. thermal features. The information obtained is integrated into a conceptual model that is combined with historical data of field production and performance to build a representation of the geothermal system, a geothermal reservoir model. This model is evaluated using constitutive equations built into a computer code, a computer simulator, which procures the simulation of fluids and heat flow from recharge to outflow areas.



Figure 1: Location map of the Wairakei-Tauhara Geothermal System (light grey shaded area), limited by its resistivity boundary at 500 mbgl (after Rosenberg et al., 2010). Black dots mark the locations of the monitored wells and samples for this study.

Petrophysical properties used in the models are often obtained from a calibration process that may over-simplify the complexity of the reservoir rocks. This study shows the adaptation and application of a rock typing technique based on textural descriptors as proxies to petrophysical properties to potentially assess reservoir-rock quality

2. MODELLING GEOTHERMAL RESERVOIRS

Reservoir models aim to reflect what is known about the geothermal system including 1) heat source and distribution capacity; 2) reservoir and cap rocks quality, i.e. capacity of rocks to store and transfer fluids; 3) physicochemical properties of fluids (e.g., phases, concentration of solids and gases) and their circulation patterns; and 4) thermodynamic conditions (temperature and pressure).

Modern geothermal simulation models are the result of a technology developed over more than four decades (Bodvarsson, Pruess, and Lippmann, 1986; O'Sullivan, Pruess, and Lippmann, 2001; Pruess, 1990; Thomas and Ray, 1978), often with input from methods developed in the petroleum and groundwater industries. Models have evolved from two blocks representing a reservoir and a recharge block (lumped-parameter models) into three-dimensional (3D) grids with multiple blocks that include spatial and temporal variation of rocks, fluids and thermodynamic parameters (distributed-parameter models).

2.1 Petrophysical reservoir characterisation

The main petrophysical parameters used in geothermal reservoirs modelling are density (ρ), porosity (ϕ), permeability (k) and thermal conductivity (λ). These parameters describe the ability of the rocks to store and transport fluids and to transfer heat. Porosity and permeability are often used to describe the quality of a reservoir by defining its storage capacity ($\phi \times$ rock thickness) and flow capacity ($k \times$ rock thickness) (Gunter et al., 1997).

Although these properties might be available from drill-core samples and electrical logs, the upscaling of the values to a reservoir scale remains poorly understood. Therefore, these parameters are often assumed as constants or calibrated by matching a modelled response of the reservoir to the historical production data, under certain assumptions and constraints.

The original manual calibration used to adjust these parameters has been rapidly replaced in the last decade by computer assisted calibration, inverse modeling (O'Sullivan et al., 2001). Still this process can be computationally intensive and typically requires manual intervention to guarantee the best representation of the system.

Experience in volcanic petroleum reservoirs (Li, Zhao, and Han, 2014) indicates the reservoir characterisation may be improved by increasing the model complexity with the appropriate integration of available measured petrophysical data and other indirect data to the modelling workflow.

2.2 Rock typing for reservoir characterisation

Conventionally, the classification of rock units for geothermal reservoir modelling in New Zealand is based on geological features such as genesis, formation age or lithology (e.g. Mannington, O'Sullivan, and Bullivant, 2004; Massiot et al., 2011; Newson et al., 2012; Pearson and Prieto, 2012; Pearson, 2012), and rarely based on their quality as reservoir- or cap-rocks. This is partially due to the lack of available measured data, but also to the high variability of petrophysical properties within a single rock unit. The variability result from diagenetic and tectonic processes that commonly change primary properties expected in unaltered rocks. These uncertainties make difficult to assign and predict parameters such as ϕ and k using conventional indexing of rock units. As an alternative, a classification of rock types based on petrophysical properties can be implemented.

There are numerous rock typing methods applied to petroleum reservoirs that are derived mainly from empirical correlations observed on core data, e.g. Winland R₃₅ in Pittman (1992), flow zone indicators FZI (Amaefule, Altunbay, Tiab, Kersey, and Keelan, 1993), global hydraulic elements GHE (Corbett and Potter, 2004).

Nevertheless, their application to New Zealand's geothermal reservoirs has been limited due to the availability of core samples and measured properties.

2.3 Textural descriptors applied to rock typing

Rock typing methods in sandstones and carbonate reservoirs have proved the utility of combining textural descriptors described on drill cores and cuttings, e.g. particle size and sorting, as representations to the pore geometry and, therefore, to the reservoir-rock quality (Archie, 1952; Lucia, 1995; Sneider, King, Hawkes, and Davis, 1983).

Considering that drill cuttings are the most common rock sample available from geothermal wells in New Zealand, this method has the potential to allow the extrapolation of rock-types between similar uncored sections.

Preliminary work undertaken by the authors on the application of rock typing techniques based on textural descriptors to volcanic rocks of New Zealand showed that observed features; including surface appearance, groundmass particle size, argillaceous content and consolidation, are practical to characterise effusive and volcaniclastic rocks; and that they display an apparent effect on measured porosity and permeability (Prieto, Mielke, Archer, and Sneider, 2015; Prieto, n.d.).

To advance our previous work, we used an additional set of samples, including effusive rocks. Here we present the textural descriptions and the observed relationships with measured porosity and permeability, followed by an example of rock types identification.

3. METHODOLOGY

3.1 Samples selection

Selected samples for this study were obtained from drilled-cores collected in five shallow monitoring boreholes of the Tauhara Geothermal Field (THF), the eastern part of the Wairakei-Tauhara Geothermal System (Figure 1).

Samples include pyroclastic (lithic- and vitric-breccias, lithic and vitric lapilli-tuffs) and volcaniclastic (sandstones and mudstones) deposits belonging to the Waiora Formation (WAF) and Huka Falls Formation (HFF); and lavas (andesitic) and autoclastic deposits (breccias) from the Spa Andesite Formation, as described by detailed geological logging (Rosenberg, Ramirez, Kilgour, Milicich, and Manville, 2009).

The Waiora Formation (ca 0.32 Ma) comprises interlayered pyroclastic, volcaniclastic and clastic units, overlying conformably the Wairakei Ignimbrites, part of the ca. 0.33-0.34 Ma Whakamaru Group ignimbrites (Brown, Wilson, Cole and Wooden, 1998), and underlying the HFF. The thickness of WAF ranges between 400m and >2,100 m, and its brecciated units comprise the main geothermal reservoirs at the TGF (Rosenberg et al., 2010).

The Spa Andesite Formation is the youngest known subsurface andesite in the TGF and consists predominantly of at least 200 m of lavas and autoclastic breccias within WAF, locally underlying HFF (Prasetyo, Browne, Zarrouk, and Sepulveda, 2012). It has a permeable zone identified close to the bottom of the unit (Rosenberg et al., 2010).

The Huka Falls Formation is generally described as three sub-units. The Upper and Lower HFF members are fine-

grained lacustrine deposits and constitute aquiclude. The Middle HFF member has been described as a sub-aqueous breccia (Cattel, 2011) and is associated to shallow aquifers. The HFF is recognised as the cap rock of the geothermal system (e.g. Mannington et al, 2004), separating the hot deep aquifers from the colder shallow ones.

3.2 Samples preparation and petrophysical analyses

Petrophysical analyses, methods and results are reported in detail by Mielke, Prieto, Bignall, and Sass, 2015.

Eighty-three (83) core plugs of 4 cm in diameter and 2 to 3 cm long were drilled, oven-dried for more than 24 hours at about 40°C, and then cooled down to room temperature. They were used to calculate effective gas permeability by using steady-state air flow in a Hassler-cell columnar permeameter.

Plug end trims of 1 to 1.5 cm long were cut off and used to evaluate bulk density and effective porosity using a gas-driven pycnometer (AccuPyc II 1340), and a displacement technique that measures volume using a quasi-fluid (GeoPyc 1360).

Subsequently, we broke the end trims apart to achieve freshly broken and dried samples. A part of them was dyed with a coloured resin (blue epoxy) and the surface was polished to better identify the 2D pore geometry. High resolution digital photomicrographs of the samples were snapped with reflective light before and after impregnation for image analyses techniques.

3.3 Textural descriptors classification

In volcanic settings such as that of Wairakei-Tauhara, textural terminology commonly used for clastic and carbonate rocks is not suitable, therefore we adapted a classification system with terms from igneous petrology literature (Table 1).

Archie's (1952) classification to describe surface appearance observed on freshly dry broken rocks at 20x magnification was followed. We described rock fabric on plugs and end-trims adapting the classification introduced by Lucia (1995) to differentiate particle- and groundmass-dominated fabrics. Cryptocrystalline particles size was set as groundmass threshold. Particle size was classified according to the Wentworth-Udden-Krumbein scale and assigned from the modal size of the dominant element, i.e. particle or groundmass. It was identified by microscopic observation with reflected light (up to 60x magnification) on plugs and end trims, and by 2D measurements of extracted objects on photomicrographs analysis using JMicroVision (Roduit, 2014). Sorting of particle-supported rocks was estimated using visual comparison charts from Beard and Weyl (1973) on end trims, and calibrated with calculations using the Folk and Ward (1957) graphical method in GRADISTAT v 8.0 (Blott, 2010). Consolidation degree was classified by observing the way the end trims broke as in Sneider and King (1984). It is considered as an indicator of rock cementation and compaction. The percentages of argillaceous content, i.e. groundmass and other pore-filling materials) was classified following Sneider (2010) and estimated using visual comparators (Folk, 1951) on plug and end trims at 20x magnification, complemented by values obtained using colour intensity thresholds and background definition in the analyses of photomicrographs of dyed samples. In a similar way we

classified visible porosity, i.e. size, volume and type of pores, but colour intensity thresholds were applied for object extracted in the image analysis.

The term “particle” is used here in the sense of Lucia (1983) to refer to crystals and grains.

After assigning a reference number to each class per descriptor (Table 1); e.g. in surface appearance, 1, 2 and 3 correspond to granular, chalky and compact textures respectively; we used cross-plots of ϕ vs. k to observe relationships between individual descriptors and hydraulic properties.

3.4 Rock types classification

The rock typing scheme we used is adapted from the methodology introduced by Sneider et al. (1983) using textural descriptors to group rocks with similar quality (Figure 2).

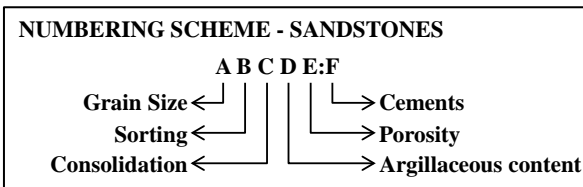


Figure 2: Example of sample number classification scheme applied to sandstones. After Sneider et al. (1983).

Each descriptor was placed in a position of a pre-determined numbering scheme (e.g. A to F in Figure 2). A number from Table 1 was assigned to each position based on the observed classes. The combined resulting numbers were sorted in ascending order and grouped together. A group of more than three samples constitutes a rock type, and each rock type represents rocks with similar rock quality.

Two examples of rock typing are given and compared with units defined by lithotypes and GHE. The first one based on petrographical descriptions, i.e., breccias, sandstones, mudstones, tuffs and lavas; and the second one, based on the systematic selection of FZI calculated from

$$FZI = (0.314 * \sqrt{k/\phi}) / (\phi/1 - \phi) \quad (\text{Amaefule et al., 1993})$$

to delimit hydraulic units.

4. RESULTS AND DISCUSSION

Cross-plots of textural descriptors and rock properties (Figure 3) suggest that some textural descriptors identified in volcanic rocks have an effect on their effective porosity and permeability and, therefore, they can be used as proxies of a rock hydraulic behavior. Additionally, we observe that by combining these textural features a classification of rocks with similar reservoir-rock quality can be achieved.

4.1 Textural descriptors in volcanic rocks

The selected textural descriptors applied on volcaniclastic and effusive rocks in this study include surface appearance, rock fabric, particle size, sorting, argillaceous content, consolidation, and volume, size and type of visible porosity.

By using cross-plots of ϕ vs. k (Figure 3) we compare the correlation between classes of textural descriptors and these two hydraulic properties. It is assumed that rocks with similar k/ϕ ratio display similar rock-quality, while comparatively higher ratios indicate higher flow capacity, hence better reservoir-rock quality.

Figure 3a presents classes of surface appearance where samples with granular textures display generally higher k/ϕ than rocks with chalky texture. Two rocks with compact texture are recognised with the lowest permeability observed. The granular appearance is related to a structure of particles that allows for open space usually increasing

the flow capacity of the rock. In contrast, the smaller and better interlocked particles of rocks with chalky texture have smaller and less interconnected pore space that results in lower permeability values.

Figure 3b shows particle-supported samples (Class 2) prevailing in the area of higher k/ϕ ratio which is comparable with observations in carbonate rocks (e.g. Lucia, 1995). Class 3 samples, although particle-supported, display low reservoir-quality as an effect of occluded porous space. Additionally, Class 4 samples show higher k/ϕ than Class 5 due to the different groundmass proportion between them.

Table 1: Classification of textural descriptors and equivalent terms conventionally used in clastic and carbonate reservoirs (after Prieto, n.d.)

TEXTURAL DESCRIPTORS	CLASSIFICATION IN VOLCANICLASTIC / EFFUSIVE ROCKS			CLASTIC/CARBONATE ROCK	
Surface appearance (SA)	1. Granular: particles interlock at different angles, visible interparticle space, sugary appearance 2. Chalky: particles <0.063 mm, not so tightly interlocked, dull and unreflective appearance 3. Compact: tightly interlocked particles, rare to none interparticle porosity, crystalline to resinous appearance			Granular	
Rock fabric (RF)	1. Particle-dominated, particle-supported with open interparticle space 2. Particle-dominated, particle-supported with interparticle space partially filled 3. Groundmass-dominated, particle-supported with filled interparticle space 4. Groundmass-dominated, groundmass-supported with >10% particle content 5. Groundmass-dominated, groundmass-supported with <10% groundmass content			Grain dominated Mud dominated	Grainstone Packstone Packstone Wackstone Mudstone
Particle size (PS)	1. Pegmatic 2. Phaneritic 3. Coarse 4. Medium 5. Fine 6. Aphanitic 7. Cryptocrystalline	Very coarse Coarse Medium Fine Very fine	>2 mm >1 - 2 mm >0.5 - 1 mm >0.25 - 0.5 mm >0.125 - 0.25 mm >0.06- 0.125 mm <0.063 mm	Gravel Sand Coarse Very coarse Medium Fine Very fine Clay-silt	Calcarudite Calcarenit
Sorting (SO)	1. Aplitic-aphanitic 2. Porphyritic 3. 4. 5.	Equigranular Moderately equigranular Inequigranular Very inequigranular Bimodal		Very well / well / moderately well Moderate Poor Very poor Bimodal	
Argillaceous content (%) (AC)	1. Clean 2. Slightly argillaceous 3. Moderately argillaceous 4. Argillaceous 5. Very argillaceous	<25 >25 - 50 >50 - 75 >75 - 80 >80		Clean Slightly shaly Moderately shaly Shaly Very shaly	
Degree of consolidation (CO)	1. Unconsolidated 2. Slightly consolidated 3. Moderately consolidated 4. Moderately well consolidated 5. Well consolidated 6. Very well consolidated			Unconsolidated Slightly consolidated Moderately consolidated Moderately well consolidated Well consolidated Very well consolidated	
Porosity volume (%) (PORV)	1. >35 2. >30-35 3. >25-30 4. >20-25	5. >15-20 6. >10-15 7. >5-10 8. <5		>35 >30-35 >25-30 >20-25	>15-20 >10-15 >5-10 <5
Pore size (PORS)	1. Micro-pores - A 2. Visible-pores-B 3. C 4. D	<0.125 mm 0.125- 2 mm >2 mm		Non-visible- A Visible B C D	<0.125 mm 0.125- 2 mm >2 mm
Porosity type (PORT)	1. Separated 2. 3. 4. Connected/Touching 5. 6. 7.	Interparticle Intraparticle Vuggy Pipe-vesicle touching Fracture Autobreccia Joint		Interparticle-intercrystalline Intraparticle-intracrystalline Moldic – vugular (isolated) Channel – vugular (touching) Fracture Breccia Shrinkage	

Particle size is one of the main descriptors that controls the geometry of the pore system (Lucia 1983). Modal classes are shown in Figure 3c and 3d for groundmass- and

particle-supported fabrics respectively. They are plotted separately to observe the effect of particle size of the supporting framework. No dominant trend is observed in

the few particle supported samples. In contrast, a dominant trend can be observed in Figure 3d of particles larger than 0.06 mm in size showing high permeability. This matches with observations of earlier studies in sandstones (Sneider

and King, 1984). Due to the small number of samples Class 5 ($>0.125 - 0.25$ mm) and to the difficult identification of particles smaller than 0.063 mm, we cannot discuss the boundaries for carbonates suggested by Lucia (1983).

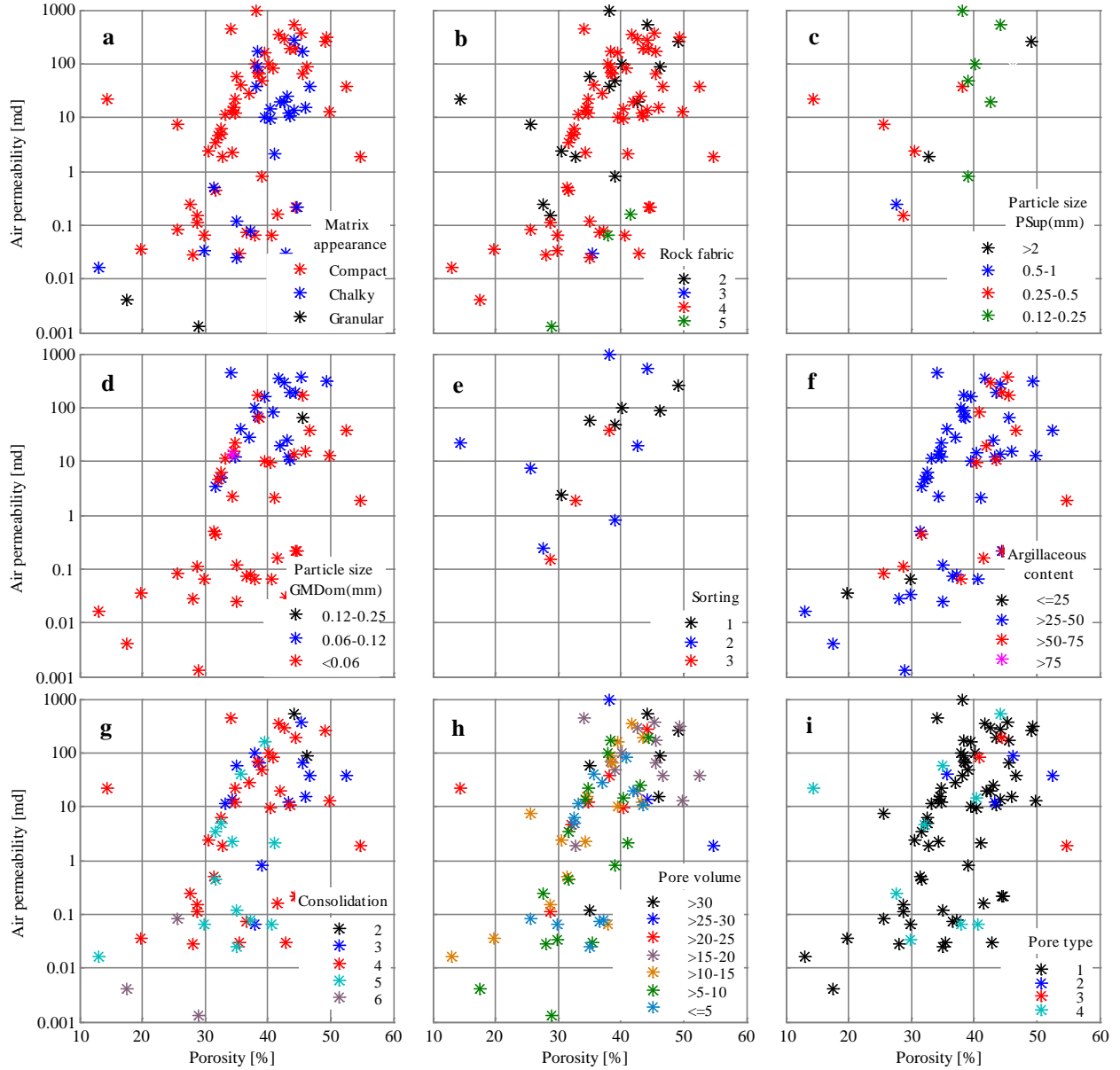


Figure 3: Effective porosity vs. air permeability cross plots comparing classes of textural descriptors (a) surface appearance; (b) rock fabrics; (c) particle size in samples with particle-supported fabric; (d) particle size in samples with groundmass-supported fabric; (e) sorting within samples with particle-supported fabric; (f) argillaceous content in groundmass-dominated samples; (g) degree of consolidation; (h) percentage of visible porosity (including B and C pore-sizes and (i) main porosity types.

Most of the studied volcanic effusive samples exhibit very porphyritic or bimodal texture with phaneritic-size particles in aphanitic to cryptocrystalline groundmass making difficult to establish significant differences using the traditional sorting classification. Consequently, no evident trend can be observed on sorting of particle-supported rocks in relation to ϕ and k (Figure 3e) as previously reported in Prieto et al. (2015). Still, the number of available samples remains too small to be considered significant.

The percentage of argillaceous content is shown in Figure 3f. Although we have not made a distinction in the

composition, e.g. volcanic glass, clays, silica; or genesis, e.g. devitrification, alteration, precipitation; of the material, samples with higher argillaceous content tend to have lower k/ϕ values and hence lower quality.

The assessment of consolidation is presented in Figure 3g showing slightly (Class 2) to very well consolidated (Class 6) rocks. Samples in classes 2 and 3 are associated with higher k values in a wide range of ϕ , while Class 6 samples display lower k . This agrees with the expected behaviour of less consolidated rocks having more favorable pore geometry to allow fluid flow. Nevertheless, no trend is

observed for rocks classes 4 and 5 which represent a high percentage of the samples. Despite the lack of a trend observed that is possibly related to the different influence of the two components of consolidation, i.e. mechanical and chemical compaction, we consider this descriptor related to the hydraulic behaviour of the rocks.

The percentage of visible porosity observed is shown at 5% intervals in Figure 3h. Only pores-sizes B and C were identified with the help of image analyses on impregnated samples. We observe pore volume increasing proportionally to φ and k , with classes 1 to 5 (PORV>15%) primarily related to higher k values (>10md) in a wide range of φ . Stronger trends were expected considering the control of visible porosity on the geometry of the pore system. Nevertheless, correlations of macro-porosity can be poor in cases where micro-porosity has a stronger influence in the pore system (Lucia, 1995).

No trends are observed related to visible porosity type (Figure 3i). Separate-interparticle porosity prevails as the main porosity type. Interconnected types, e.g. touching vugs, do not present an increase of flow capacity as it is expected, and separate-intraparticle and -vugs appear to display higher φ and k . The lack of correlation is also associated to a stronger control of micro-porosity in the pore system.

Some challenges in the descriptions are exposed in Prieto et al. (2015). We emphasize that acceptable estimates of textural descriptors obtained by using visual comparators on hand specimens are only achieved with practice and consistency, but provides a fast assessment especially useful for on-site descriptions while drilling. Additionally, a combination of different types of samples, e.g. cores, plugs, photomicrographs; and analysis techniques, e.g. microscopic examination, image analyses; contributes with acquiring more precise estimates.

The previous descriptions confirm the correlation of textural descriptors with measured porosity and permeability, and show their utility to give indication of the hydraulic behavior of rocks. Nevertheless, additional textural descriptors relevant to high-temperature geothermal settings are to be included in future work.

4.2 Rock typing

Following two numbering schemes, we sorted the samples and grouped them by numbers, assigning a rock type to groups of more than three samples as illustrated in Table 2.

Table 2: Rock types generated using textural descriptors Rock Fabric, Argillaceous Content and Surface Appearance.

Sample	RF	AC %	SA	Rock type No.	Rock type Class	Phi	k
E2_7	4	2	1	421	3	32.1	4.7
E3_1	4	2	1	421	3	36.6	0.1
A3_1	4	2	1	421	3	34.8	21.6
F2_3	4	2	2	422	4	43.4	12.3
F2_2	4	2	2	422	4	44.1	13.8
A2_3	4	2	2	422	4	38.4	173.8
B1_3	4	3	1	431	5	40.7	81.9
D1_3	4	3	1	431	5	45.3	365.4
C1_3	4	3	1	431	5	42.5	289.3

As a way of comparison, the studied samples are also classified by lithotypes (Figure 4a) and GHE (Figure 4b). It

can be observed that, in general, mudstones and lavas display low k values and a wide range of φ . On the contrary, tuffs display high k values also with scattered φ . Sandstones and breccias, although with predominantly high k , display widespread φ . The high dispersion observed makes it difficult to establish ranges for φ and k as predictors using this classification system. In contrast, classes of GHE assigned based on calculated FZI represent well defined units with similar specific ranges of hydraulic properties. However, to obtain FZI values measured values of φ and k are required but are not often available in geothermal reservoirs.

Figure 4c shows rock types defined by combining rock fabric (RF), argillaceous content (AC) and surface appearance (SA) (corresponding to A, B and C in Figure 2) GHE boundary lines are plotted as reference in dark grey. The resulting classes show very high dispersion. Yet, types 3, 4 and 5 are distributed within two or three adjacent GHE. Figure 4d combines RF, AC, SA and particle size (PS). We observe that with the addition of one descriptor to the numbering scheme the dispersion is reduced, resulting in most classes limited to two adjacent GHE.

The combination of textural descriptors that optimally represent patterns of the hydraulic behaviour of the rocks and the adequate thresholds to discretise rock units will be studied in future work by using computational models, e.g. artificial neural networks.

With these examples, we illustrate the use of textural descriptors and measured petrophysical properties in volcanic rocks to determine rock types. With the potential of recognising these textures also in drill cuttings, a rock typing system can be propagated to un-cored sections of wellbores enhancing the use of measured properties in the reservoir modelling workflow.

5. CONCLUSIONS

Porosity and permeability are petrophysical parameters important to describe the ability of the rocks to store and transport fluids. Yet, they remain poorly understood at a reservoir scale as they are difficult to predict and assign to conventionally indexed rock units, e.g. geological formations. This difficulty is mainly related to the high spatial variability observed in such properties due to secondary processes which modify primary rock properties of unaltered rocks.

By applying a rock typing method used in petroleum reservoirs, we described selected textural descriptors on hand samples. As a result we observed subtle correlations between four descriptors: surface appearance, rock fabric, predominant particle size and argillaceous content, and measured effective porosity and permeability values. We conclude that these descriptors can be used as proxies of reservoir-rock quality in volcanic rocks.

Furthermore, we combined these descriptors into numbering schemes to show the principles of rock typing. Despite the dispersed of the results, they provide a range of properties that is difficult to obtain from lithotypes, and that can be contained within hydraulic units given by GHE.

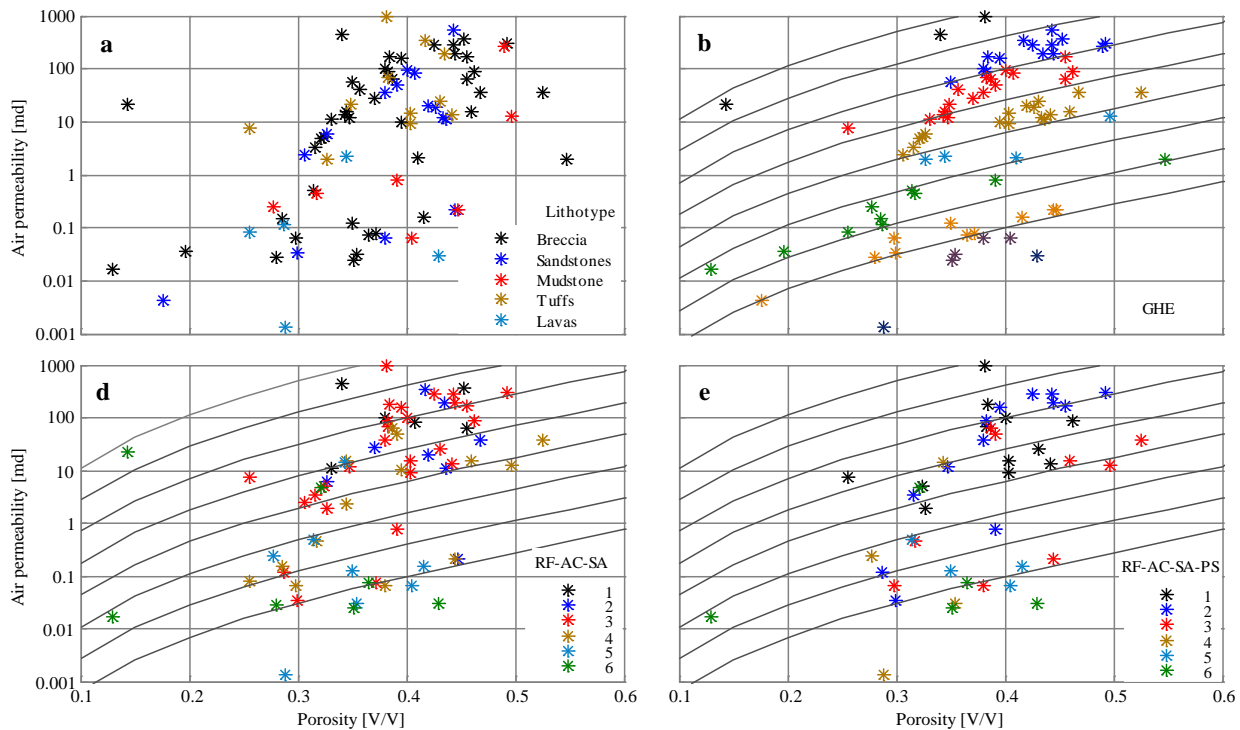


Figure 4: Effective porosity vs. air permeability cross plots comparing samples classified by (a) lithotypes; (b) global hydraulic elements (GHE); (c) rock types derived from rock fabric (RF), argillaceous content (AC) and surface appearance (SA) descriptors, (d) rock types derived from rock fabric (RF), argillaceous content (AC), surface appearance (SA) and particle size (PS) descriptors. Continuous lines represent boundaries of hydraulic units given by pre-defined FZI.

This method has the potential to allow the extrapolation of values of petrophysical properties between rock types defined by similar textural features observed in hand samples including drill cuttings, the most common rock sample available from geothermal wells in New Zealand.

ACKNOWLEDGMENTS

This research was supported through The University of Auckland Geothermal Institute by funds of the Mighty River Power Chair in Geothermal Reservoir Engineering, the Technische Universität Darmstadt and GNS Science 'Geothermal Resources of New Zealand' Core Science Area research programme. The authors thank Contact Energy Limited for their authorization to use their core material.

REFERENCES

AccuPyc II 1340. [Apparatus]. Micromeritics. <http://www.micromeritics.com/product-showcase/accupyc-ii-1340.aspx>. (2014).

Amaefule, J. O., Altunbay, M., Tiab, D., Kersey, D. G., and Keelan, D. K. Enhanced reservoir description: using core and log data to identify hydraulic (flow) units and predict permeability in uncored intervals/wells: SPE 26436. *Proc. 68th Annual Technical Conference and Exhibition of the Society of Petroleum Engineers*, Houston, Texas, USA. (1993).

Archie, G. E. Classification of carbonate reservoir rocks and petrophysical considerations. *AAPG Bulletin*, 36(2), 278–298. (1952).

Beard, D. C., and Weyl, P. K. Influence of texture on porosity and permeability of unconsolidated sand. *AAPG Bulletin*, 57(2), 349–369. (1973).

Blott, S. J. *Gradistat Version 8.0*. [Computer software]. Berkshire, UK. (2010).

Bodvarsson, G. S., Pruess, K., and Lippmann, M. J. Modeling of geothermal systems. *Journal of Petroleum Technology*, 1007-1021. (1986).

Bromley, C. J. New Zealand Country Report. In *2012 GIA Annual Report*. Retrieved from <http://iea-gia.org/wp-content/uploads/2013/10/2012-NZCountry-Report-IEA-GIA-with-Cover-Photo-16Oct13-pdf.pdf>. (2012).

Brown, S. J. A., Wilson, C. J. N., Cole, J. W., and Wooden, J. The Whakamaru group ignimbrites, Taupo Volcanic Zone, New Zealand: evidence for reserve tapping of a zoned silicic magmatic system. *Journal of Volcanology and Geothermal Research*, 84, 1-37. (1998).

Cattell, H.J. *Subaqueous Eruption Breccia of the middle unit of the Huka Falls Formation, Tauhara Geothermal System, Taupo Volcanic Zone*. (Honour's Project). University of Canterbury, New Zealand. (2011).

Corbett, P. W. M., and Potter, D. K. Petrotyping: a basemap and atlas for navigating through permeability and porosity data for reservoir comparison and permeability prediction. *Proc. International Symposium of the Society of Core Analysts*. Abu Dhabi. pp.1–12. (2004).

Folk, R. L. A comparison chart for visual percentage estimation. *Journal of Sedimentary Petrology*, 21(1), 32–33. (1951).

Folk, R. L., and Ward, W. C. Brazos River Bar: a study in the significance of grain size parameters. *Journal of Sedimentary Petrology*, 27(1), 3–26. (1957).

GeoPyc 1360 [Apparatus]. Micromeritics. <http://www.micromeritics.com/Product-Showcase/GeoPyc-1360-Envelope-Density-Analyzer.aspx>. (2014).

Gunter, G. W., Finneran, J. M., Hartmann, D. J., and Miller, J. D. Early determination of reservoir flow units using an integrated petrophysical method. *Proc. SPE Annual Technical Conference and Exhibition*. San Antonio, Texas, USA. pp. 1–8. (1997).

Li, L., Zhao, H., and Han, X. Rock physical experimental research in Tanan volcanic rock reservoir. *Journal of Applied Mathematics and Physics*, 02(06), 284–295. doi:10.4236/jamp.2014.26034. (2014).

Lucia, F. J. Petrophysical parameters estimated from visual descriptions of carbonate rocks: a field classification of carbonate pore space. *Journal of Petroleum Technology*, 35(March), 629–637. (1983).

Lucia, F. J. Rock-fabric/petrophysical classification of carbonate pore space for reservoir characterization. *AAPG Bulletin*, 79(9), 1275–1300. doi:10.1306/7834D4A4-1721-11D7-8645000102C1865D. (1995).

Mannington, W. I., O'Sullivan, M., and Bullivant, D. P. Computer modelling of the Wairakei–Tauhara geothermal system, New Zealand. *Geothermics*, 33(4), 401–419. doi:10.1016/j.geothermics.2003.09. 009. (2004).

Massiot, C., Bignall, G., Alcaraz, S., Moerkerk, H. Van, Sepulveda, F., and Rae, A. The history of Ohaaki Geothermal Field - in 3D. *Proc. 35th New Zealand Geothermal Workshop*, Auckland, New Zealand. pp. 21–24. (2011).

Mielke, P., Prieto, A. M., Bignall, G., and Sass, I. Effect of hydrothermal alteration on rock properties in the Tauhara Geothermal Field, New Zealand. *Proc. World Geothermal Congress 2015*, Melbourne, Australia. (2015).

Ministry of Business Innovation and Employment. *Energy in New Zealand 2013*. Wellington: Author. (2013).

Newson, J., Mannington, W., Sepulveda, F., Lane, R., Pascoe, R., Clearwater, E., and Sullivan, M. J. O. Application of 3D modelling and visualization software to reservoir simulation: Leapfrog Geothermal and Tough2. *Proc. 37th Workshop on geothermal reservoir engineering*, Stanford, California, USA. (2012).

O'Sullivan, M. J., Pruess, K., and Lippmann, M. J. State of the art of geothermal reservoir simulation. *Geothermics*, 30(4), 395–429. doi:10.1016/S0375-6505(01)00005-0. (2001).

Pearson, S. C. P. Modeling the effects of direct use on the Tauranga Low-Temperature Geothermal System , New Zealand. *GHC Bulletin*, (May 2012), 10–17. (2012).

Pearson, S. C. P., and Prieto, A. M. Improved visualization of reservoir simulations: geological and fluid flow modeling of a high-temperature geothermal field in New Zealand. *Proc. TOUGH Symposium*, Berkeley, California, USA. pp. 1–5. (2012).

Pittman, E. D. Relationship of porosity and permeability to various parameters derived from mercury injection-capillary pressure curves for sandstone. *The American Association of Petroleum Geologists Bulletin*, 76(2), 191–198. (1992).

Prasetyo, I. M., Browne, P. R. L., Zarrouk, S. J., and Sepulveda, F. Petrology and hydrothermal alteration of the Spa Andesite from the Wairakei-Tauhara Geothermal System, Taupo Volcanic Zone, New Zealand. *Proc. 36th New Zealand Geothermal Workshop*. Auckland, New Zealand. (2012).

Prieto, A. M. *Rock typing: petroleum geology applications on geothermal reservoirs of New Zealand*. [Science Report]. Manuscript in preparation. (n.d.).

Prieto, A. M., Mielke, P., Archer, R., and Sneider, J. S. Rock typing in geothermal reservoirs, a textural approach. *Proc. World Geothermal Congress 2015*. pp. 19–25. Melbourne, Australia. (2015).

Pruess, K. Modeling of geothermal reservoirs: fundamental processes, computer simulation and field applications. *Geothermics*, 19(1), 3–15. (1990).

Roduit, N. *JMicroVision: image analysis toolbox for measuring and quantifying componentes of high-definition images*. [Computer software]. Retrieved from <http://www.jmicrovision.com>. (2014).

Rosenberg, M. D., Ramirez, L. E., Kilgour, G. N., Milicich, S. D., and Manville, V. R. *Tauhara Subsidence Investigation Project: Geological Summary of Tauhara Wells THM12-18 and THM21-22 and Wairakei Wells WKM14-15*. (2009/309) [Consultancy report]. Wairakei: GNS Science. (2009).

Rosenberg, M., Wallin, E., Bannister, S., Bourguignon, S., Sherburn, S., Jolly, G., ... Links, F. *Tauhara Stage II Geothermal Project: Geoscience report*. (2010/138 [Consultancy report]. Wairakei: GNS Science. (2010).

Sneider, J. S. *Integration of rocks, logs and test data*. Tulsa: Petroskills. (2010).

Sneider, R. M., and King, H. R. Integrated rock-log calibration in the Elmworth Field-Alberta - Part I. In J. A. Masters (Ed.), *Elmworth - Case Study of a Deep Basin Gas Field. Memoir 38* (pp. 205–214). Tulsa: American Association of Petroleum Geologists. (1984).

Sneider, R. M., King, H. R., Hawkes, H. E., and Davis, T. B. Methods for detection and characterization of reservoir rock , Deep Basin gas area , Western Canada. *Journal of Petroleum Technology*, (September), 1725–1734. (1983).

Thomas, L. K., and Ray, G. Three-dimensional geothermal reservoir simulation: SPE 6104. *Proc. SPE-AIME 51st Annual Fall Technical Conference and Exhibition*, New Orleans, USA. pp. 151–161. (1978).

Wilson, C. J. N., Houghton, B. F., Mcwilliams, M. O., Lanphere, M. A., Weaver, S. D., and Briggs, R. M. Volcanic and structural evolution of Taupo Volcanic Zone, New Zealand : a review. *Journal of Volcanology and Geothermal Research*, 68(95), 1–28. (1995).